

Studying Land Cover Change of Thermokarst Features Across the National Petroleum Reserve of Alaska Using Supervised Classification Methods

James Loken

Department of Resource Analysis, Saint Mary's University of Minnesota, Winona, MN 55987

Keywords: Alaska, Esri, GeoSpatial Services, Ice Wedge Polygon, National Petroleum Reserve Alaska, NPRA, Supervised Classification, Thermokarst

Abstract

Due to an accumulation of man-made greenhouse gas emissions, the world's climate has begun to change rapidly in the last 100 years. This new global climate shift has sent ripples across every ecosystem on earth. This shift has been especially prevalent in the continuous permafrost regions of the north above the Arctic Circle. These permafrost-rich areas can rapidly degrade, disrupting whole ecosystems and releasing greenhouse gas emissions long trapped under the permafrost at a rate unforeseen by prior studies. This study used supervised classification methods to conduct an overall land cover change in thermokarst features across a study area within the National Petroleum Reserve Alaska (NPRA). This study focused on determining if accelerated degradation can be detected using an automated classification of high-resolution satellite imagery. The methodology in this study utilized two sets of satellite imagery, MAXAR Digital Globe captured between 2010-2020 and SPOT5 captured between 2009-2013, to discern any accelerated change. The supervised classification process was performed using the Esri classification wizard in ArcGIS Pro. The study found the MAXAR Digital Globe classification had a difference of -11% in Non-thermokarst Feature coverage, 5% High-Center Ice Wedge Polygon, 3% Low-Center Ice Wedge Polygon, -2% Thermokarst Lake, -1% Open Water, 0% Ice, and 8% Beaded Streams compared to the SPOT5 classification. The study's accuracy was investigated using a confusion matrix based on 200 randomly generated check sites across each classification output. The MAXAR Digital Globe classification had an overall accuracy of 60%, and the SPOT5 classification had a 53% overall accuracy. Overall, the results were inconclusive due to the lack of accuracy in the classification. If accuracy was improved, more meaning could be concluded. In addition, an improved output could serve as a baseline for future studies of permafrost and climate change studies in the NPRA.

Introduction

This study explored an overall landscape-level coverage change of thermokarst features across the National Petroleum Refuge Area of Alaska to determine possible accelerated climate change through supervised image classification methods. Davis (2001) defined the term

thermokarst as topographic depressions created by the thawing of ground ice (Davis). Thermokarst profoundly affects not only the local ecosystem but the environment as a whole, releasing greenhouse gas emissions and disrupting overall ecosystems at an unfathomable rate (Schuur and Abbott, 2011).

Background

Climate change in the arctic is leading to widespread loss of permafrost and wide-scale ecosystem alteration (Balser, Gooseff, Jones, and Bowden, 2009). Rises in global temperatures since the 1970s have caused a rapid deterioration of permafrost across the entire Arctic Circle (Osterkamp, 2007). This deterioration has led to an abundant increase in recorded thermokarst features across the Northern slope of Alaska (Gooseff, 2009). This deterioration has led to a multitude of different formations appearing across the land, many in the form of flooded lakes, sinkholes, and collapsed hillsides (Jorgenson, Shur, and Osterkamp, 2008). These features disrupt the natural ecosystems and wreak havoc on water flow paths (Gooseff, 2009).

Project Value and Importance

Climate change in the arctic leads to widespread loss of permafrost and wide-scale ecosystem alteration (Balser *et al.*, 2009). Referencing Van Cleve and Viereck; 1983 and Ford; 1987, Jorgenson *et al.* (2008) state permafrost is an integral component of many northern ecosystems because it supports the ground surface, modifies micro topography, and influences soil temperature and moisture, subsurface hydrology, rooting zones, and nutrient cycling. Loss of these precious ecosystems could bring unimaginable consequences to the environment as a whole (Jorgenson *et al.*, 2008)

In addition, Schuur and Abbott (2011) state carbon released into the atmosphere from permafrost soils will accelerate overall climate change. They go on to state that, by their calculations, the permafrost thaw could release the same magnitude of carbon as deforestation at its

current rate (Schuur and Abbott). But because these emissions also include significant portions of methane, the overall effect on the climate would be 2.5x greater (Schuur and Abbott). By their estimation, the amount of carbon released by the thawing of permafrost by the year 2100 will be 1.7-5.2 times larger than reported in several modeling studies (Schuur and Abbott).

Study Area

The study area is located above the Arctic Circle in the National Petroleum Refuge of Alaska (NPRAs) (Figure 1).

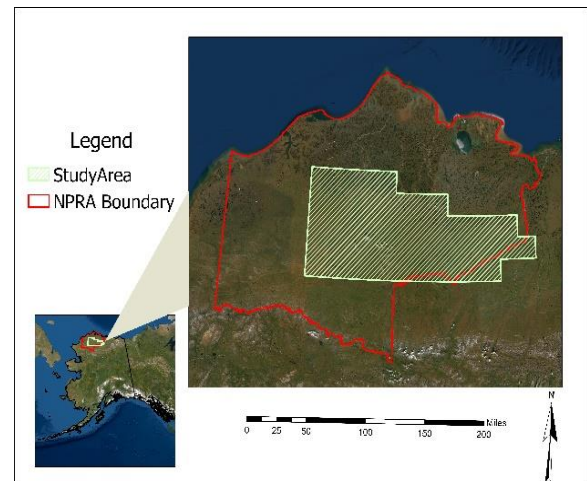


Figure 1. An overview of the project Study area. This area is located on the North Slope of Alaska within the NPRAs.

The study area is approximately 7.9 million acres in size. The shape of the project area is based on USGS 63k Quadrangles. This study area was chosen for multiple reasons. First is its significance as a resource. According to the Bureau of Land Management's (BLM) website, the NPRAs is one of the United States' largest untapped petroleum reserves containing 6.7-15 billion barrels of known oil (BLM, n.d.). The second is its importance to wildlife. These lands are vital breeding habitats for migratory

waterfowl. In addition, according to the Alaska Department of Fish and Game (ADFG), the Western Arctic and Teshekpuk caribou herds migrate through this area every year (ADFG, n.d.). Lastly, the study area was chosen for its rich abundance of thermokarst features, in particular ice-wedge polygons. Davis (2001) states an ice wedge is an ice feature that is formed in permafrost from surface water running into small cracks created by thermal contractions. Davis continues, ice-wedge arrays are widespread in permafrost, covering an estimated 10% of the northern slope of Alaska (Davis, 2001).

Project Overview

To assess the change in the overall coverage of thermokarst features in the NPRA, supervised classification methods were utilized. These methods were performed on two sets of satellite imagery. These classifications were then compared for overall change.

Summary

This study examined current geospatial techniques to identify thermokarst features across the NPRA. Supervised classification was utilized to identify thermokarst features across the study area. These classification outputs were analyzed for overall land coverage. In addition, the classification outputs were assessed for accuracy and compared for significant change.

Methods

The methodology outlined in the following paragraphs details supervised classification using the classification wizard toolset. The toolset used is

included in the Esri ArcGIS Pro Image Analyst extension. In addition, an assessment was performed on the training data and the classification output. Finally, the classification outputs were analyzed.

Data

Due to the lack of available data in Alaska, a limited amount of data was utilized. This study used two sets of multispectral satellite imagery as the primary data source for the classification process. The first image set acquired was SPOT5 tiles across the NPRA (Figure 2). This set of imagery has a resolution of 2.5 meters by 2.5 meters. In addition, each image tile is a 3-band color infrared (CIR) image. The image tiles located within the study area were captured between 2009 and 2013 in the spring season based on metadata. The SPOT5 image tiles were acquired through Saint Mary's University of Minnesota GeoSpatial Services. An alternative web mapping service (WMS) is available online through the GeoNorth Information Systems website.

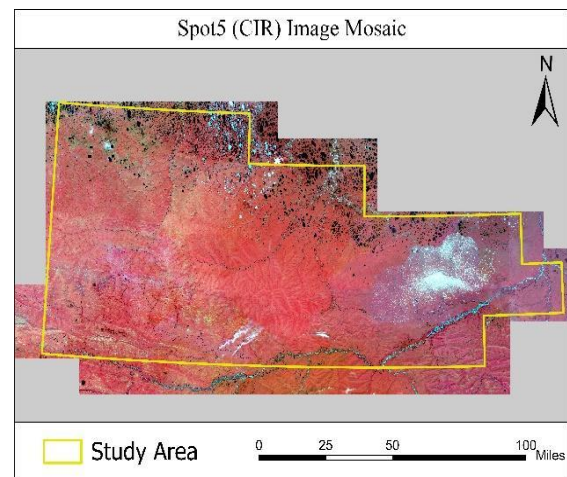


Figure 2. An overview of the SPOT5 satellite image set.

The second image set acquired for classification was MAXAR Digital Globe tiles (Figure 3). This set of imagery has a

resolution of 50 cm by 50 cm. In addition, each image tile consists of 4-bands. The image tiles were captured from 2010 through 2020 during the spring season based on metadata. The MAXAR digital globe image set has a resolution 50 times more detailed than the SPOT5 image set. The MAXAR image tiles were acquired through Saint Mary's University of Minnesota GeoSpatial Services. An alternative web mapping service (WMS) is available online through the State of Alaska Open Data Geoportal website.

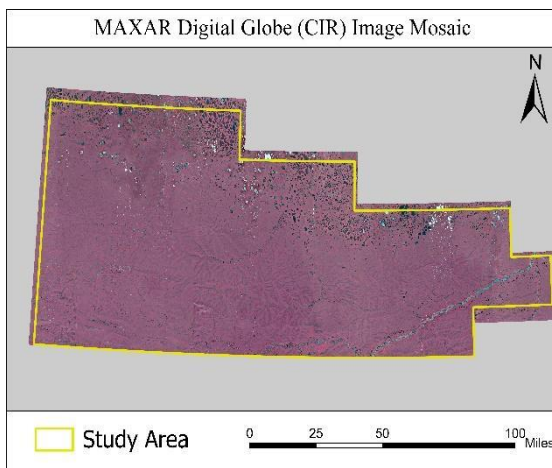


Figure 3. An overview of the MAXAR Digital Globe image set.

After the individual image tiles for each set were downloaded, Esri's ArcCatalog was used to create Mosaic datasets for each imagery set. These mosaic datasets were used in the classification process. Both mosaic image sets cover the entirety of the study area.

Classification Process

The Esri ArcGIS Pro classification wizard was utilized to classify both sets of imagery. This wizard uses a multi-step workflow (Figure 4).

The first step of the classification wizard is image segmentation. Esri defines image segmentation as the process by which neighboring pixels are grouped by

similarity in color and shape characteristics (Esri, n.d.). This process is a crucial component of the classification workflow because the rest of the classification can be skewed based on the parameters provided in this step. The three parameters for this step were spectral detail, spatial detail, and minimum segment size. Spectral detail is the level of importance given to spectral differences in the imagery when processing. The higher the value, the higher the level of detail distinguished in the output. Spatial detail is the level of importance given to the proximity between the features in the image set. The higher the value, the smaller the cluster of pixels is in the output. Finally, the minimum segment size determines how small a feature can be. If the feature or pixel group is under the threshold, they are merged into the nearest neighboring feature. Both spectral and spatial detail were left at their default values of 15, respectively. The defaults were appropriate because they allowed for a high level of detail to be discerned without significantly increasing the overall processing time. The minimum segment size was increased to 1000 to account for the overall density of pixels in the Digital Globe image set. Because of the minuscule size of each pixel, if the minimum was not raised, the end results could be skewed. The minimum segment size used for the Spot5 classification was left at the default value of 100.

Step two of the classification process was to create training sample data that are used to train the classification algorithm. First, a classification schema was created. The classes defined were Open Water, Non-Thermokarst, Beaded Stream, Thermokarst Lake, High-Center Ice Wedge Polygon, and Low-Center Ice Wedge Polygon. These classes were based on

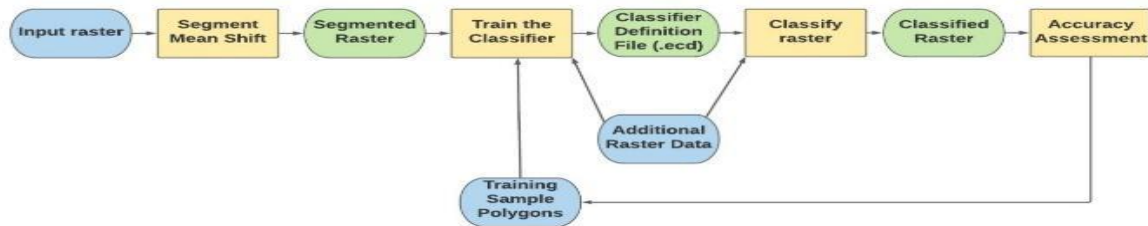


Figure 4. Workflow diagram of the supervised classification wizard workflow.

the twenty-two different thermokarst features outlined by Jorgenson *et al.* (2008). Of the twenty-two outlined, these four types of thermokarst features, along with the other classes Ice, Open Water, and Non-Thermokarst features were the most prevalent and discernable features in the study area. The classes were used to collect sample polygons correlating to a feature in the imagery. Training sample areas were created in 3 sections of various 63k quadrangles scattered across the study area (Figures 5, 6, and 7). These training areas were chosen to be a representative sample of the entire study area with each containing some features from each class. The first area is located in the homogenous rolling hills that cover a majority of the study area. The second area was located on the Arctic coastal plain. The third and final area was located along the Coleville River. Delineation of the training polygons was performed at a scale of 1:6000k. Digital Globe was used for preliminary sample data delineation. The results of the delineation of sample data in the three training areas selected (Figures 8, 9, 10, 11, and 12). An assessment was performed both visually and in the field to verify the accuracy of the training samples created. Based on the field assessment, these training samples were further refined to increase classification accuracy.

The third step of the supervised classification process is training the classifier. This step uses the segmented image from the first step and the training data created in the previous step. The

classification method used was Support Vector Machine or SVM. SVM is an advanced machine learning classification method. This method is less susceptible to noise, band shift, and unbalanced training sites per class. These are issues because they can all skew the final classification and increase overall error across the classification output. SVM is the preferred classification method recommended by Esri documentation (Esri n.d.).

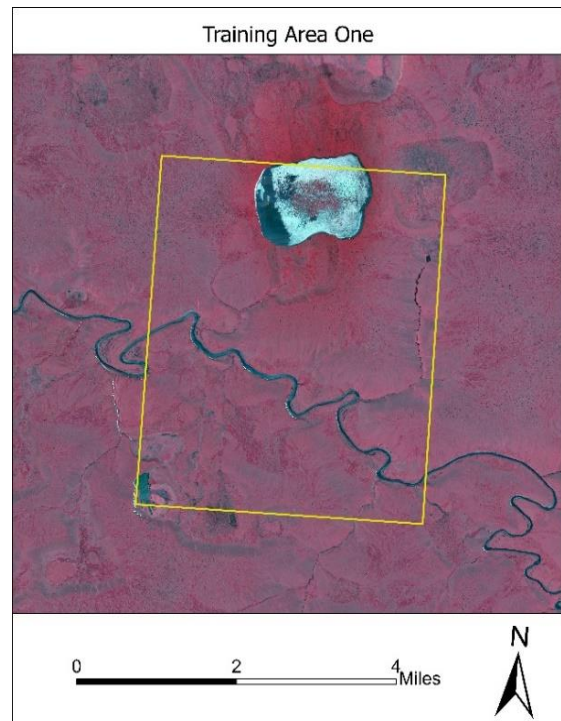


Figure 5. An overview of training area one. This area was delineated to train the image classifier. The dark features in the imagery are open water features, either lakes or rivers. The white signature is remaining ice. The reddish color is a matrix of emergent vegetation and small shrubs.

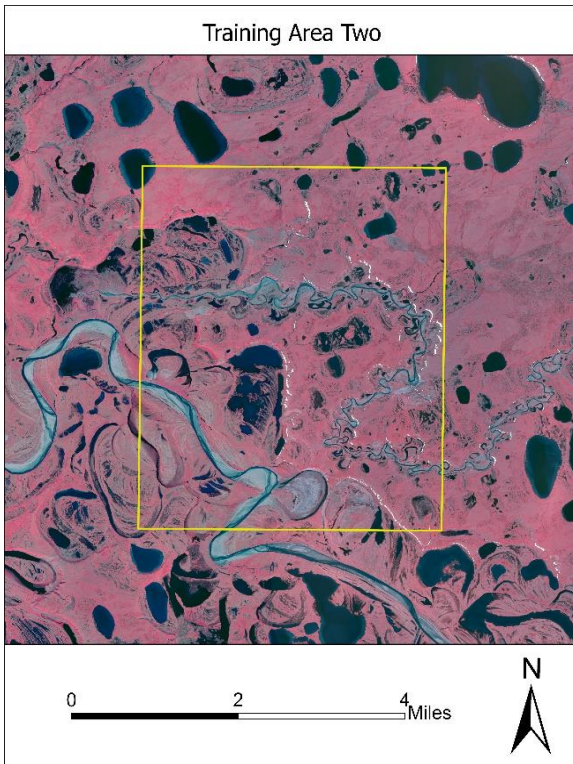


Figure 6. An overview of training area two. This area was delineated to train the image classifier.

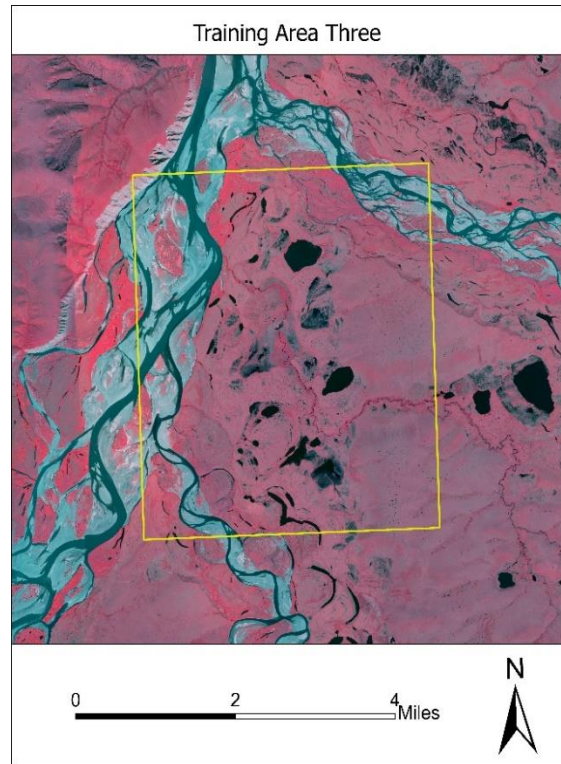


Figure 7. An overview of training area three. This area was delineated to train the image classifier.

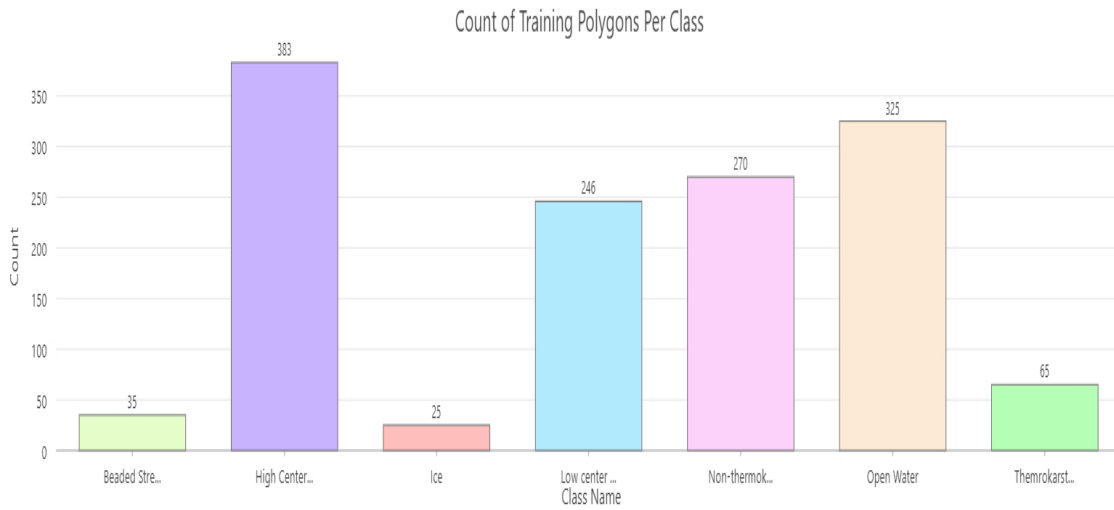


Figure 8. Graphic displaying the number of training polygons captured for each class. This graph represents all polygons delineated across all three training areas.

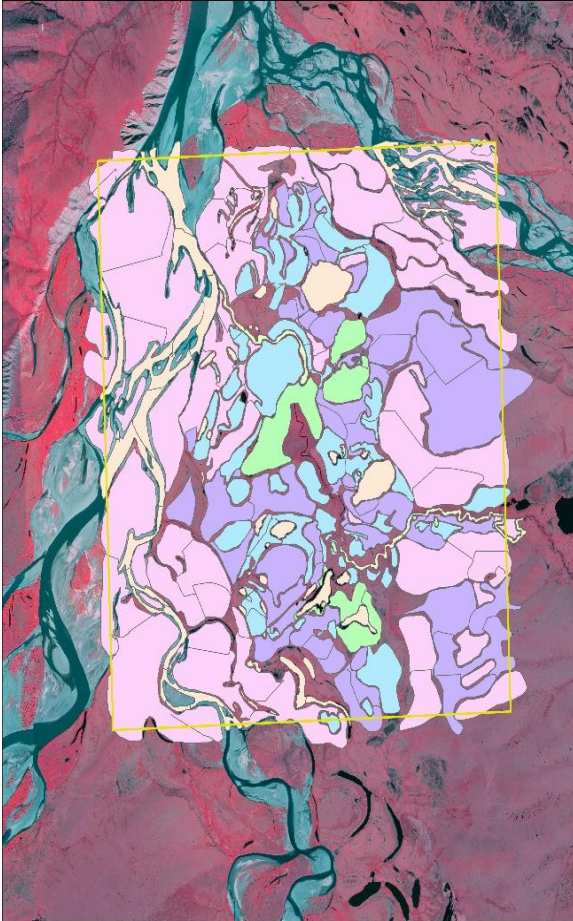


Figure 12. Sample data delineated in training area three. Every individual polygon is left separated to make it easier to make changes to each shape based on the accuracy assessment performed later in the study.

The fourth step of the classification process was to run the classifier. The classifier used all the data created in the previous actions. The output of this step was the final image classification.

The final step of the classification wizard is to run the built-in accuracy assessment provided by Esri. This built-in evaluation uses a stratified random strategy to compare classes with a ground reference. With this evaluation, areas of concern were reclassified to the correct class.

The classification process was performed on both the SPOT5 and the MAXAR Digital Globe mosaics. The

same parameters were entered for both sets of imagery for each step of the classification wizard. To ensure the accuracy of the classification process, multiple types of accuracy assessments were performed on each output.

Accuracy Assessment

Two different methods were employed to assess the accuracy of the classification results—the first was Esri’s recommended image classification assessment workflow. The second was field verification of preliminary results and training data used in the classification process.

Accuracy assessment is an essential part of the classification process. To assist with this task, Esri’s accuracy assessment workflow for ArcGIS Pro was utilized. This workflow uses two geoprocessing tools: Create Accuracy Assessment Points and Compute Confusion Matrix. This workflow allows for an easy method for reviewing outputs between classification runs and overall accuracy at the end of the classification process. Create Accuracy Assessment points generates randomly sampled points across a given classification. Each point contains a corresponding classification value and a ground truth value of -1. The ground truth value was updated for every assessment point based on interpretation of the MAXAR Digital Globe and SPOT5 image sets. Once each classification’s points ground-truth value was updated, the Compute Confusion Matrix tool was used. This tool took the updated accuracy points and computed a confusion matrix comparing the classification results to the ground truth values. The confusion matrix displays errors of omission and commission and derives a kappa value that indicates overall classification accuracy. This process was run on both the SPOT5

and MAXAR Digital Globe classification outputs. In addition to a visual assessment, field verification was also performed on preliminary data.

Field verification of the initial classification and training data set was performed in early July 2021. This verification was conducted from an r44 raven helicopter flying at roughly 2500 ft. During field verification, two tasks were completed. The first was to verify the training sample data produced for the classification process. The training data was delineated and verified using the MAXAR Digital Globe image set. This step was accomplished by creating check sites in Esri ArcGIS Pro that would be input into the pilot's GPS. Four check sites were verified in two of the three training areas. The accuracy of placement, signature, and class designation were verified. In addition, verification was performed on a preliminary classification of the Digital Globe image set. The classification output was compared on a handheld laptop running ArcGIS Pro to the corresponding features below the helicopter. This verification was completed while visiting the check sites in each training area. Verification photos were captured at most check sites and flight lines for reference.

Statistical Analysis

Finally, a statistical analysis was performed to derive meaning from the data. Each classification raster was split into eight areas to improve processing speed. These eight splits were roughly equal in size. Then, each area was converted from raster format into a polygon feature class using Esri's ArcGIS Pro built-in conversion tool. The polygon features were merged together to create one comprehensive data set for each

classification.

Statistics were run on these converted areas to determine each category's total coverage in both classification outputs. These totals were then compared for differences in spatial distribution. This workflow is highlighted below (Figure 13).

Results

Classification Results

This study focuses on the overall land cover change in thermokarst features between the MAXAR Digital Globe and SPOT5 satellite image sets. The general shift in land coverage of thermokarst features was assessed by measuring the total area of each class in both classification outputs and comparing the results. The shape area of each converted polygon feature was used to determine the entire area for each category. In addition, accuracy assessments were performed on each of the classification outputs.

SPOT5 Classification Result

The SPOT5 supervised image classification results are as follows (Figure 14 and Table 1). The results can be seen in each class's percentage of coverage and total area.

MAXAR Digital Globe Classification Result

The MAXAR Digital Globe supervised image classification results are as follows (Figure 15 and Table 2). The results can be seen in each class's percentage of coverage and total area. The difference is highlighted below (Table 3). The numbers in red represent a negative change.

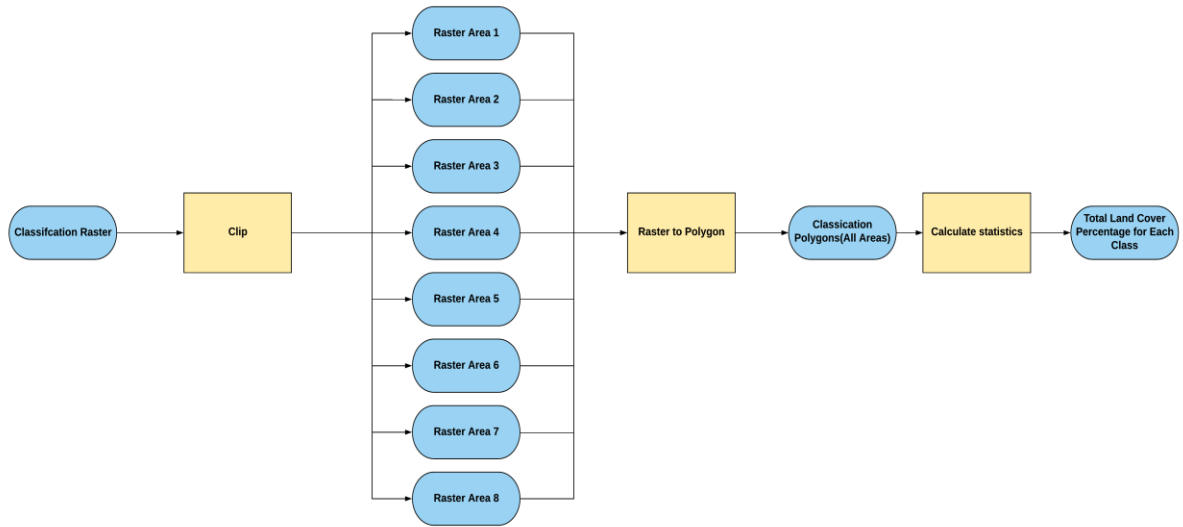


Figure 13. A workflow diagram detailing the process used to convert each classification output into a more interpretable form. This process was run on both the SPOT5 and MAXAR Digital Globe classification outputs.

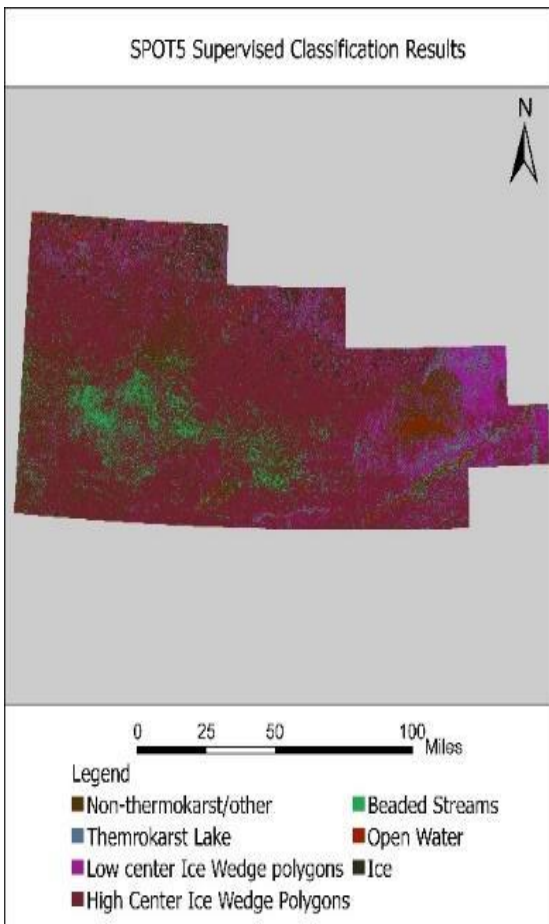


Figure 14. The results of the SPOT5 supervised classification process.

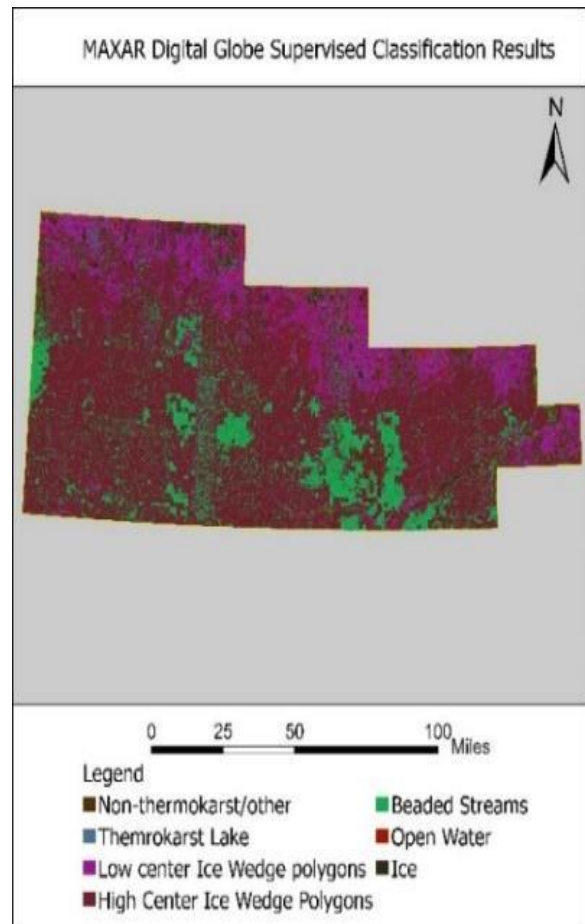


Figure 15. The results of the MAXAR Digital Globe supervised classification process.

Table 1. Total area of each class for the MAXAR Digital Globe classification output. Each class has a corresponding area coverage in acreage and total percent coverage of the entire study area.

Total Area Based on Classification Category for MAXAR Digital Globe		
Class	Area(Acres)	Percent coverage
Non-thermokarst Feature	433,122	5%
High Center Ice wedge Polygon	4,550,875	58%
Low Center Ice Wedge Polygon	1,052,401	13%
Thermokarst Lake	165,499	2%
Open Water	193,623	2%
Ice	206,061	4%
Beaded Stream	1,306,875	17%

Table 2. Total area of each class for the SPOT5 classification output. Each class has a corresponding area coverage in acreage and total percent coverage of the entire study area.

Total Area Based on Classification Category for SPOT5		
Class	Area(Acres)	Percent coverage
Non-thermokarst Feature	1,181,368	16%
High Center Ice wedge Polygon	3,977,235	53%
Low Center Ice Wedge Polygon	764,384	10%
Thermokarst Lake	300,162	4%
Open Water	247,592	3%
Ice	282,491	4%
Beaded Stream	627,109	9%

Table 3. The difference in total land coverage of thermokarst features between MAXAR Digital Globe and SPOT5 Satellite Imagery across the project study area. The numbers in parentheses represent a negative change.

The Total Difference of Thermokarst Feature Land Coverage Between MAXAR Digital Globe and SPOT5 Satellite Image Sets Based On Supervised Classification							
	Class						
	NON	HCIW	LCIW	TL	OW	IC	BS
Digital Globe	5%	58%	13%	2%	2%	4%	17%
SPOT5	16%	53%	10%	4%	3%	4%	9%
Difference	(11%)	5%	3%	(2%)	(1%)	0%	8%

Accuracy Assessment Results

Kappa Values

Kappa values ranging from 0.4 to 0.6 have

a weak level of agreement, with 15-35% of the data produced being reliable. A value ranging from 0.6 to 0.8 has a moderate level of agreement, with 35-63% of the data being reliable. A value between

0.8 and 0.9 would have a strong level of agreement, with 64-81% of the data being reliable. Finally if the kappa value is above 0.9, the level of agreement is almost perfect, and there is between 82 and 100% reliability in the data.

Digital Globe Classification Assessment

The Esri image classification assessment results for the MAXAR Digital Globe classification are as follows (Table 4).

The overall accuracy of the classification was 60%. The bold numbers running diagonal represent the correctly classified pixels for each class. The kappa value derived was 0.42.

SPOT5 Classification Assessment

The Esri image classification assessment

results for the SPOT5 classification are as follows (Table 5).

The overall accuracy of the classification was 53%. The bold numbers running diagonal represent the correctly classified pixels for each class. The kappa value derived was 0.28.

In the Field Assessment

An in-the-field assessment was performed on a preliminary classification attempt in July of 2021. During this fieldwork, two training areas were assessed. Only two training areas were able to be evaluated based on time and budget constraints.

In each region, four points were assessed for accuracy in both the training data and classification.

Table 4. MAXAR Digital Globe classification Confusion Matrix. The diagonal number represents how many objects were correctly classified. In the bottom right is the overall accuracy of the classified output and the kappa value.

MAXAR Digital Globe Classification Accuracy Assessment Confusion Matrix										
Class Value	Non-Thermokarst Features	Thermokarst Lake	Low Center Ice Wedge Polygons	High Center Ice Wedge Polygons	Beaded Streams	Open Water	Ice	Total	User Accuracy	Kappa Value
Non-Thermokarst Features	4	0	0	1	0	0	1	6	67%	0
Thermokarst Lake	0	6	2	0	0	2	0	10	60%	0
Low Center Ice Wedge Polygons	4	1	8	9	0	0	0	22	36%	0
High Center Ice Wedge Polygons	14	0	2	62	0	1	0	79	78%	0
Beaded Streams	5	0	0	15	2	2	0	24	8%	0
Open Water	0	0	0	0	0	10	0	10	100%	0
Ice	1	0	1	1	1	2	4	10	40%	0
Total	28	7	13	88	3	17	5	161	0%	0
Producer's Accuracy	14%	86%	62%	70%	67%	59%	80%	0%	60%	0
Kappa Value	0	0	0	0	0	0	0	0	0	0.423511265

Table 5. SPOT5 classification Confusion Matrix. The diagonal number represents how many objects were correctly classified. In the bottom right is the overall accuracy of the classified output and the kappa value.

SPOT5 Classification Accuracy Assessment Confusion Matrix										
Class Value	Non-Thermokarst Features	Thermokarst Lake	Low Center Ice Wedge Polygons	High Center Ice Wedge Polygons	Beaded Streams	Open Water	Ice	Total	User Accuracy	Kappa Value
Non-Thermokarst Features	11	0	1	9	0	0	5	26	42%	0
Thermokarst Lake	3	2	2	0	0	0	0	7	29%	0
Low Center Ice Wedge Polygons	8	0	2	5	2	0	1	18	11%	0
High Center Ice Wedge Polygons	20	0	2	72	0	0	0	94	77%	0
Beaded Streams	5	1	0	7	0	0	0	13	0%	0
Open Water	0	0	1	0	0	5	2	8	63%	0
Ice	0	0	0	0	0	8	0	8	0%	0
Total	47	3	8	93	2	13	8	174	0%	0
P. Accuracy	23%	67%	25%	77%	0%	38%	0%	0%	53%	0
Kappa Value	0	0	0	0	0	0	0	0	0	0.284919561

This assessment was performed on a handheld Toshiba Toughbook computer running ArcGIS Pro. In each area, field photos were collected, documenting each site and immediate surrounding area.

Area One

Point One

The first point was placed directly over an open water lake in the MAXAR Digital Globe imagery. The classification identified the area as open water (Figure 16).



Figure 16. Aerial field photo of the first accuracy assessment point in the first training area. A large open body of water.

Point Two

The second point in this area is in the middle of a high-center ice wedge polygon flat adjacent to a low-center ice wedge polygon area based on the MAXAR Digital Globe imagery. The classification identified the site as a low-center ice wedge polygon (Figure 17).

Point Three

The third point in the first area was located in the floodplain of a river. This area would constitute a non-thermokarst

feature. The classification identified the site as non-thermokarst (Figure 18).



Figure 17. Aerial field photo of the second accuracy assessment point in the first training area. There is a large plain of high-center ice wedge polygons adjacent to regions of low-center polygons and open water features.



Figure 18. Aerial field photo of the third accuracy assessment point in the first training area. Tundra plains along a river. This area consists of non-thermokarst features.

Point Four

The fourth and final point selected in area one is located in a large river floodplain on a riparian island near the center of the channel. This area is non-thermokarst based on the MAXAR Digital Globe imagery. The classification identified this area as non-thermokarst (Figure 19).



Figure 19. Aerial field photo of the fourth accuracy assessment point in the first training area. A sandbar island located along a major river. This area consists of non-thermokarst features.

Area Two

Point One

The first point in the second area was located in a patch of shrub-covered high-center ice wedge polygons. The classification identified the area as high-center ice wedge polygon (Figure 20).



Figure 20. Aerial field photo of the first accuracy assessment point in the second training area. Tussock-covered high-center ice wedge polygons.

Point Two

The second point in the second area was placed on a non-thermokarst slope near a river. The classification identified the area as a mix of high-center ice wedge polygon and non-thermokarst features (Figure 21).



Figure 21. On the ground photo of the second accuracy assessment point in the second training area. A non-thermokarst region adjacent to a river.

Point Three

The third point in the second area is in the middle of a high-center ice wedge polygon flat adjacent to a sizeable ice-covered lake based on the MAXAR Digital Globe imagery. The classification identified the site as a low-center ice wedge polygon (Figure 22).



Figure 22. On the ground photo of the third accuracy assessment point in the second training area. Tussock-covered high-center ice wedge polygons.

Point Four

The fourth and final point in the second area is in a group of high-center ice wedge polygons based on MAXAR digital globe imagery. The classification identified it as a high-center with regions of low-center

ice wedge polygons surrounding it (Figure 23).



Figure 23. Aerial field photo of the fourth accuracy assessment point in the second training area. High-center polygons with flooded low-center borders.

Discussion

This section details discussion on the classification process results, accuracy assessment results, errors in the data, data limitations, and future recommendations.

Classification

The goal to utilize supervised image classification to discern a landscape-level change in thermokarst feature coverage worked in some ways and not in others. The MAXAR Digital Globe classification output had 16% total coverage of Non-thermokarst Feature, 53% High-Center Ice Wedge Polygon, 10% Low-center Ice Wedge Polygon, 4% Thermokarst Lake, 3% Open Water, 4% Ice, and 9% Beaded Stream. The SPOT5 classification output had 5% total coverage of Non-thermokarst Feature, 58% High-Center Ice Wedge Polygon, 13% Low-Center Ice Wedge Polygon, 2% Thermokarst Lake, 2% Open Water, 4% Ice, and 17% Beaded Stream. The MAXAR Digital Globe classification had a difference of -11% in Non-thermokarst Feature coverage, 5% High-Center Ice Wedge Polygon, 3% Low-

Center Ice Wedge Polygon, -2% Thermokarst Lake, -1% Open Water, 0% Ice, and 8% Beaded Stream compared to the SPOT5 classification. The MAXAR Digital Globe accuracy assessment results gave the classification an overall accuracy of 60%. The SPOT5 classification had an overall accuracy of 53%.

Due to the low accuracy in both classifications, it is hard to draw any significant conclusion from the comparison. However, the methods and workflows outlined in this paper can be refined and improved upon to increase overall accuracy further. If an accurate classification is produced, the output can serve as a baseline for future studies of similar nature focusing on climate change.

Digital Globe Confusion Matrix

The confusion matrix generated for the MAXAR Digital Globe classification gave the output an overall accuracy of 60%. The table also provides a kappa value of 0.42. Since the kappa score is between 0.4 and 0.6, there is a weak level of agreement between the imagery and classification output. These values can be increased by refining the training data provided to the classifier.

SPOT5 Confusion Matrix

The confusion matrix generated for the SPOT5 classification gave the output an overall accuracy of 53%. The table also provides a kappa value of 0.28. Since the kappa score is between 0.2 and 0.4, there is a minimal level of agreement between the imagery and classification output. These values can be increased by refining the training data provided to the classifier.

Fieldwork Assessment

Four sites were assessed for two training areas. The results of the assessment from the first area were 4/4 or 100% accuracy. The results of the second area were 2/4 or 50%. Due to lack of time and funding, more points could not be assessed, but more assessment points would need to be visited to increase overall meaning.

Classification Errors

Errors in both classifications were prevalent along seams in adjacent image tiles and tiles captured at different times of the year. These errors led to a significant decrease in overall accuracy. Examples of these errors occur across both classification outputs (Figures 24 and 25).

Accuracy Assessment Errors

Due to the size of each classification, only 200 field points were generated to compute each confusion matrix. To increase overall quality in the assessment, more points would need to be visited and ground-truthed.

Data Limitations

Imagery

The imagery used had some limitations that became apparent during the data processing stage. These limitations were color balancing and seam lines between image tiles in each mosaic, overlapping years of imagery, and varying resolution. Color balancing to standardize each color band's spectral signature across all image tiles for the entire state was performed on both imagery sets. Issues can be seen in adjacent tiles where ground-truthed areas appear to be the same feature but have wildly different spectral signatures. In addition, the edge of some image tiles,

depending on when the adjacent tile was captured, had a visible seam. At times this presented as ice covering half a lake or abrupt change in signature across tiles. These limitations skewed the overall result in both classifications and led to errors in both outputs (Figure 26 and 27).

Another limitation of the imagery was the overlapping acquisition dates from 2010-13 between both image sets. Due to the lack of available image sets for the study area, SPOT5 and MAXAR Digital Globe were utilized for the classification. This overlap in acquisition could skew the comparison, but the individual classification outputs remain true.

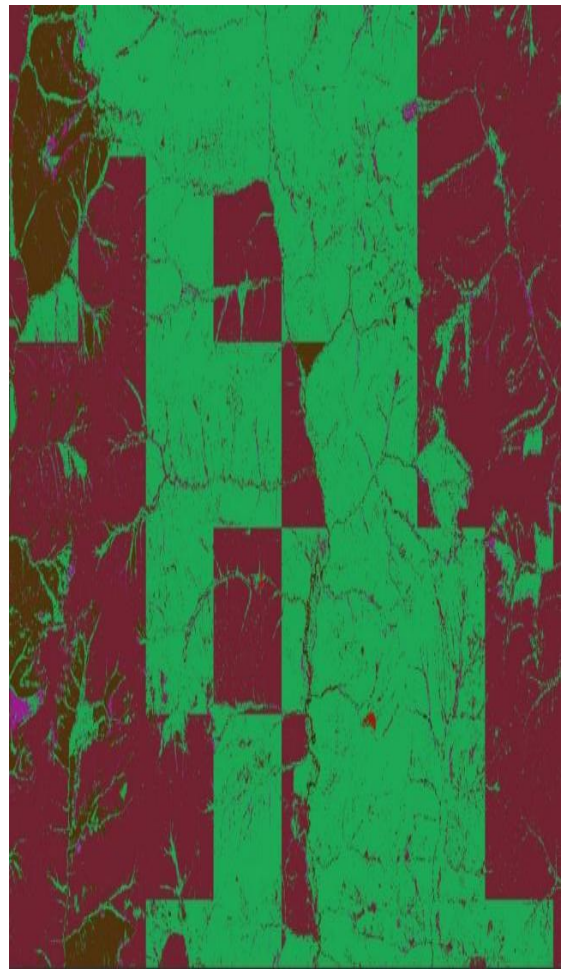


Figure 24. An example of a common error found in the MAXAR Digital Globe classification output.



Figure 25. An example of an error is due to adjacent image tiles being captured at different points of the year. The area on the right is covered in snow, while the left has none.

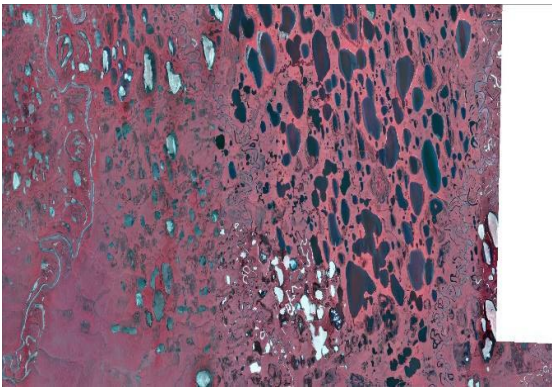


Figure 26. An example of both spectral and seasonal differences in adjacent image tiles in the MAXAR Digital Globe image mosaic

In addition to spectral errors, another limitation of the imagery were varying resolutions. The SPOT5 image set

had a resolution of 2.5 meters by 2.5 meters, while the MAXAR digital globe set had a resolution of 50 cm by 50 cm. This is 50 times more resolution than the SPOT5 data set. Due to this drastic difference in resolution, the SPOT5 classification could be skewed since the training data used to train the classifier was delineated using the MAXAR Digital Globe image set.

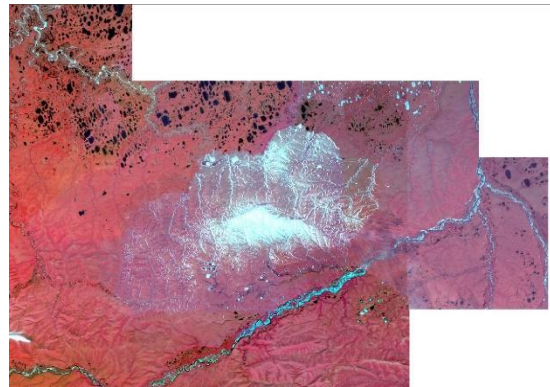


Figure 27. An example of both spectral and seasonal differences in adjacent image tiles in the SPOT5 image mosaic.

The final limitation of the imagery that might have skewed the results was the band number/ordering difference. The Spot5 Image set has three bands Red, Blue, and Green. The Spot5 image tiles were received pre-processed for color infrared or CIR, so the RGB bands of each image tile are not true to the original image. In contrast, the MAXAR Digital Globe set has four bands, RGB with an additional Alpha band. These image tiles were received in true color form. The bands had to be changed to achieve CIR with the Digital globe set. Red was changed to the Alpha band, Green was changed to the Red band, and Blue was changed to the Green band. This transformed the true color image tiles into CIR tiles like the SPOT5 tiles. CIR was utilized to make identifying wetlands and open water signatures easier when delineating training data.

Size of Data

The size of the data ended up being a significant limitation, limiting the number of trial runs available. The MAXAR Digital globe mosaic has an uncompressed size of 730 gigabytes. The SPOT5 mosaic is 100 gigabytes in size. The spot classification output size was 95 gigabytes, and the SPOT5 output was 6 gigabytes in size. Due to the large size of these files, processing times took exponentially longer than expected. For example, the classification process on the MAXAR Digital Globe image set took 10-12 days of 24 hour non-stop processing. Due to these data limitations, only a few classifications attempts were performed for each image set.

Recommendations for Future Studies

To improve overall classification results in future studies, several different methods should be employed. The first is to increase the number of training areas delineated. Due to time constraints, only a few areas were delineated for training data. If more data were given to the classifier, a more accurate output would potentially be produced. The second recommendation is to incorporate Interferometric Synthetic Aperture Radar (IFSAR) elevation to segment areas of known features. For example, most ice-wedge polygons, high and low-center, occur on low slope flats either at the top or bottom of the rolling hills of the tundra based on field observations. If areas of higher slope were masked out, potentially a more accurate output could be produced.

Conclusions

In conclusion, this study's main objective was to identify possible accelerated

climate change through supervised classification of thermokarst features. This study identified thermokarst features in two sets of satellite imagery using the supervised classification of two image sets. The MAXAR Digital Globe classification had a difference of -11% in Non-thermokarst Feature coverage, 5% High-Center Ice Wedge Polygon, 3% Low-Center Ice Wedge Polygon, -2% Thermokarst Lake, -1% Open Water, 0% Ice, and 8% Beaded Streams compared to the SPOT5 classification. The MAXAR classification had an overall accuracy of 60%, and the SPOT5 classification had a 53% overall accuracy. Due to low overall accuracy in the classifications used for comparison, no conclusions could be drawn. If overall accuracy was improved, more meaning could be concluded. In addition, an improved output could serve as a baseline for future studies permafrost studies in the NPRA.

Acknowledgments

I would like to acknowledge the following people and institutions:

Dr. John Ebert and Greta Poser for their guidance with not only this project but during my time enrolled in the Data Intelligence and GeoAnalytics program at Saint Mary's University of Minnesota.

Jeffery Knopf for assisting with the classification process and answering any questions I had while processing my data.

Andy Robertson and the Geospatial services staff provided me with both sets of satellite imagery used in this study. In addition, they allowed me to perform fieldwork on the North Slope this past July.

References

Alaska Department of Fish and Game. n.d.

- Caribou species Profile. Retrieved November 8, 2021 from <https://www.adfg.alaska.gov/index.cfm?adfg=caribou.main>.
- Balsler, A.W., Gooseff, M.N., Jones, J.B., and Bowden, W.B. 2009. Thermokarst distribution and relationships to landscape characteristics in the Feniak Lake region, Noatak National Preserve, Alaska. *Arctic Network*, 1-12. Retrieved January 24, 2021 from GeoSpatial Services Fileserver.
- Bureau of Land Management (BLM). n.d. National Petroleum Reserve in Alaska. Retrieved November 8, 2021 from <https://www.blm.gov/programs/energy-and-minerals/oil-and-gas/about/alaska/NPR-A>.
- Davis, N. 2001. *Permafrost A Guide to Frozen Ground in Transition*. Fairbanks, AK: University of Alaska Press. Retrieved January 24, 2021.
- Esri. n.d. Image Segmentation. Retrieved November 8, 2021 from <https://pro.arcgis.com/en/pro-app/latest/help/analysis/image-analyst/segmentation.htm>.
- Gooseff, M. 2009. Effects of Hillslope Thermokarst in Northern Alaska. *EOS*, 90, 1-3. Retrieved January 24, 2021 from GeoSpatial Services Fileserver.
- Jorgenson, M.T., Shur, Y.L., and Osterkamp, T.E. 2008. Thermokarst in Alaska. *Ninth International Conference On Permafrost*, 869-876. Retrieved January 24, 2021 from GeoSpatial Services Fileserver.
- Osterkamp, T.E. 2007. Characteristics of the recent warming of permafrost in Alaska. *Journal of Geophysical Research*, 112, 1- 10. Retrieved January 24, 2021 from GeoSpatial Services Fileserver.
- Schuur E., and Abbott, B. 2011. High risk of permafrost thaw. *Nature*, 480, 1-2.
- Retrieved January 24, 2021 from GeoSpatial Services Fileserver.